J Mol Model (2008) 14:39–48
DOI 10.1007/s00894-007-0249-9

ORIGINAL PAPER

A study on antimalarial artemisinin derivatives using MEP maps and multivariate QSAR

Fábio José B. Cardoso · Antonio Florêncio de Figueiredo · Maycon da Silva Lobato · Ricardo Moraes de Miranda · Ruth Catarine O. de Almeida · José Ciríaco Pinheiro

Received: 3 March 2007 / Accepted: 4 October 2007 / Published online: 30 October 2007

Abstract Artemisinin and some derivatives with activity against D-6 strains of *Plasmodium falciparum* were studied. Molecular electrostatic potential (MEP) maps were used in an attempt to identify key features of the compounds that are necessary for their activities, and then use those to propose new artemisinin derivatives. The partial least squares (PLS) method was then used to generate a predictive model. The PLS model with three latent variables explaining 88.9% of total variance, with Q^2= 0.839 and R^2=0.935, was obtained for 15/6 compounds in the training/external validation set. For construction of the model, the most important descriptors were the highest occupied molecular orbital (HOMO) energy, atomic charges on the atoms O1 (Q_1) and C3 (Q_3), molecular volume (VOL), and hydrophilic index (HYF). From a set of 20 proposed artemisinin derivatives, one new compound (**39**) with higher antimalarial activity than the molecules initially studied was predicted. Synthesis of these new derivatives may follow the results of the MEP maps studied and the PLS modeling.

Keywords Artemisinin derivatives · *Plasmodium falciparum* · Molecular electrostatic potential · MEP maps · Partial least squares modeling

F. J. B. Cardoso · A. F. de Figueiredo · M. da Silva Lobato · R. M. de Miranda · R. C. O. de Almeida · J. C. Pinheiro (✉)
Laboratório de Química Teórica e Computacional,
Departamento de Química, Centro de Ciências Exatas e Naturais,
Universidade Federal do Pará,
CP 101101, 66075-110 Belém, PA, Amazônia, Brazil
e-mail: ciriaco@ufpa.br

Introduction

Malaria is the major cause of death among the world's population in tropical regions of the planet. Most deaths are attributed to the parasite *Plasmodium falciparum*. The severity of the disease caused by this species results primarily from its ability to modify the surface of infected red blood cells by inserting proteins [1]. The enzymes in the parasite digestive vacuole (cysteine- and aspartic-proteinases) break down hemoglobin into amino acids and heme [2]. While all the amino acid content is used to build parasite proteins, only a small portion of the heme is incorporated into the parasite hemoproteins; the rest of the heme is detoxified (polymerized) by parasite enzymes [3]. A number of drugs have been investigated for their use in the treatment of malaria [4–7]. However, new strains of *Plasmodium falciparum* resistant to some of those drugs are causing substantial deterioration in clinical treatment [4–7]. This has motivated the search for new antimalarial drugs that are effective against this form of malaria, having thus a very high priority in antimalarial drug design [8–10]. This led to Chinese researchers introducing a new compound, qinghaosu (or artemisinin, as it is known in the West), present in extracts of Qinghao or *Artemisia annua L.* that have been used in China for thousands of years [11]. The structure of artemisinin was identified as an endoperoxide containing sesquiterpene lactone (Fig. 1, compound **1**) and the presence of the 1,2,4-trioxane-ring system seems to be essential for its antimalarial activity [12–16]. Studies on the mode of action of artemisinin and its derivatives have shown that free heme could be the molecule targeted by artemisinin in biological systems and that Fe^{+2} ions interact with the peroxide when artemisinins react with heme [8, 10, 17–20]. An initial step in the action of artemisinin includes heme-catalyzed artemisinin activation into a very reactive

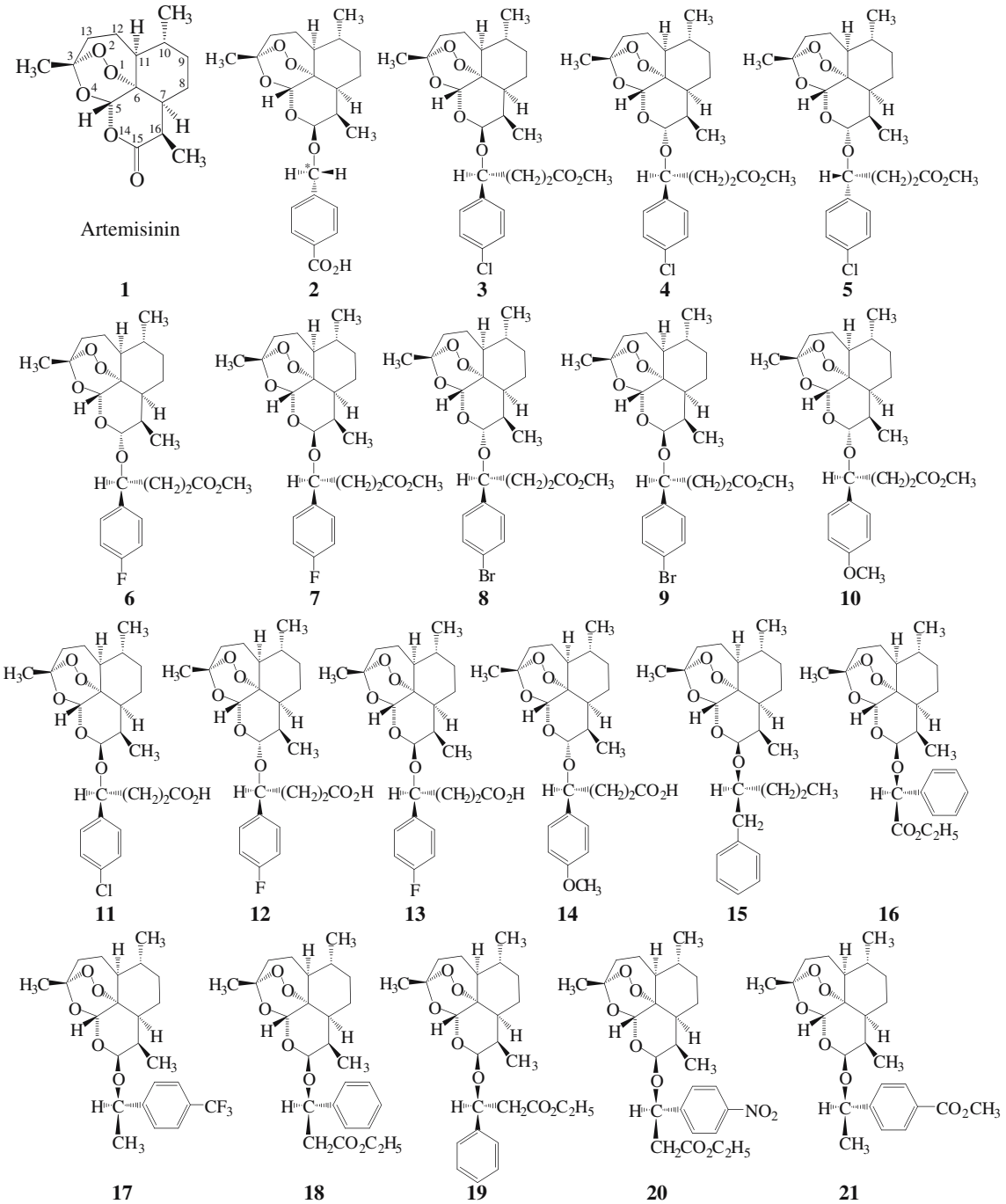

Fig. 1 Artemisinin and derivatives with antimalarial activity against D-6 strains of *Plasmodium falciparum*

radical, and the subsequent covalent binding of this radical to parasite proteins or heme [4, 10, 18–21], hemozoin [4, 18–22], reduced glutathione [4, 18–23] or other parasite molecules. On the other hand, experimental studies by Hynes and coworkers [24, 25] have demonstrated that the biological activity of artemisinin derivatives is not always related to their chemical reactivity.

In a systematic study of the structure of artemisinin and related molecules, Bernardinelli et al. [12] showed that active molecules have similar molecular electrostatic potential (MEP) around the essential trioxane ring, and that this property is due to the peroxide linkage. Using the methodology of Bernardinelli et al., it is not possible to quantify the activities of the molecules studied, and so establish a quantitative comparison among those activities.

In a previous study, molecular graphics and modeling have supported partial least squares (PLS) results, revealing heme–ligand and protein–ligand stereoelectronic relationships as important factors in the antimalarial activity of artemisinin derivatives [26]. In this study, using an HF/3-

21G approach [27, 28], we built MEP maps to a training set of 21 active compounds (artemisinin and derivatives) against D-6 strains of *P. falciparum* from Sierra Leone that are resistant to mefloquine reported in the literature [29, 30] (Fig. 1), and 20 derivatives proposed by us (shown in Fig. 2, test set). The MEP maps were then evaluated and used in an attempt to identify key features of the derivatives that are necessary for their activities [12]. The PLS method [31–33] was then used to generate a predictive quantitative structure–activity relationship (QSAR) model.

Materials and methods

Computers, software, and compounds

The molecular calculations for this work were performed on an IBM-RISC-6000 machine and the statistical treatment was carried out on a PC Pentium IV computer.

In the molecular modeling step, the starting point was the construction of the structure of artemisinin (**1**) with the aid of GasussView software [34]. Complete geometry

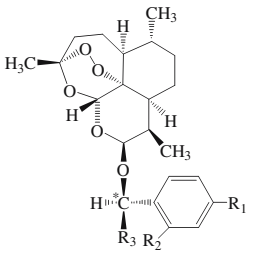

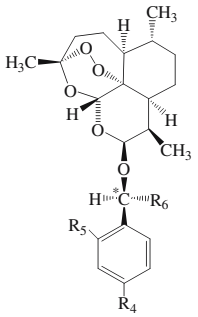

	Substituents		
Compounds	R_1	R_2	R_3
22	-CHO	-H	$-CO(CH_2)_2CO(CHOH)_2CO_2H$
23	-COCl	-H	$-(CH_2)_3CONHC_2H_5$
24	$-NO_2$	$-CF_3$	$-(CH_2)_2CH(OH)CH(OCH_3)(CO_2C_2H_5)$
25	$-COCH_3$	-F	$-(CH_2)_2CH(CO_2CH_3)_2$
	R_4	R_5	R_6
26	$-NO_2$	-Br	$-COCH_2CH(OH)CH(OCH_3)(CO_2C_2H_5)$
27		-H	$-(CH_2)_2C(CH_3)C(CO_2CH_3)_2$
28	-CHO	-F	$CO(CHOH)_2CO_2C_2H_5$
29	$-CCl_3$	-H	$C(OH)(CH_2)_4CONH(CH_2)_2CO_2H$
30	$-SO_3H$	-H	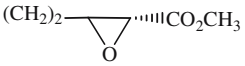
31	$-NO_2$	-Cl	$CO(CH_2)_2CO_2H$
32	$-NO_2$	-Cl	$CH_2CH(OCH_3)(CH_2)_2CO_2C_2H_5$
33	$-NO_2$	-F	$CO(CH_2)_2CH(OH)CONH_2$
34	-CN	-F	
35	$-NO_2$	$-NO_2$	$(CH_2)_2CH(CH_3)(OH)CH(OCH_3)(CO_2CH_3)$
36	$-CO(CH_2)_2CO_2H$	-H	$COCH_2CH(OH)CH(OCH_3)(CO_2C_2H_5)$
37		-H	$(CH_2)_2CH(CO_2CH_3)_2$
38	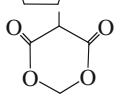	-H	$-CH_2CH(OCH_3)(CH_2)_2CO_2C_2H_5$
39		-H	$-CH_2CH(OCH_3)(CH_2)_2CO_2C_2H_5$
40		-H	
41	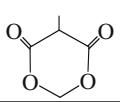	-H	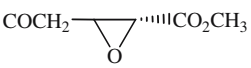

Fig. 2 New proposed artemisinin derivatives with unknown antimalarial activity against D-6 strains of *P. falciparum*

optimization was carried out with the HF/3-21G method (in this work). In order to check the reliability of the geometry obtained, we compared the structural parameters of the artemisinin 1,2,4-trioxane ring with theoretical [35] and experimental [36, 37] values from the literature. All calculations reproduced most of the structural parameters of the artemisinin 1, 2, 4-trioxane ring seen in X-ray structures (Table 1). This applies especially to the bond length of the endoperoxide bridge which, as mentioned before, seems to be responsible for the antimalarial activity [12–16]. All the other structures (Figs. 1, 2) were built with the optimized geometry of the artemisinin, also using GaussView software. Complete geometry optimizations of these molecules were carried out using the Gaussian 98 program and the DIRECT-SCF method [38].

According to the literature, when we compare artemisinin with its derivatives, the MEP maps of active compounds are similar in form to that of artemisinin in the region of the 1,2,4-trioxane ring [12]. Figure 3 shows that compounds **1**–**21** have a region of negative electrostatic potential of similar form near the trioxane ring, which indicates that all the compounds in the training set are active. This evidence is supported by the experimentally determined activity values shown in Table 2 (see blelow). Using this premise, and chemical intuition, we introduced substitutes in the artemisinin derivatives of the training set (Fig. 1) designed to maintain the antimalarial activity in the new derivatives shown in Fig. 2. The compounds in Fig. 1 were obtained from the literature [29, 30] and those which had a small methyl group substituted at the α-methylene carbon (*C) showed weaker activity than compounds with a larger carbethoxyalkyl substituent, indicating that steric effects of these molecule plays an important role in their antimalarial activity. However, we can infer that compounds (**3** – **14**) are 2- to 10-times more potent than artemisinin. In general, compounds containing chloride atoms (Cl) or bromide (Br) are more potent than analogous ones containing fluoride (F) or a methoxyl group (OCH_3), thus indicating that electronic effects may play an important role in the efficacy of these compounds. Compounds (**15**–**21**) are 3- to 9-times more potent than artemisinin; compounds containing electron-withdrawing groups such as O_2CH_3 and NO_2 substituted in the aromatic ring are more potent than analogous compounds in which the NO_2 group is absent. All the activities used in this article are logarithms of relative activity (RA) (RA = IC_{50} of artemisinin/IC_{50} of analogue). For each new derivative we built a corresponding MEP map and compared its form with those of compounds **1**–**21** in the region near the trioxane ring.

The MEP maps were computed from the electronic density and displayed using MOLEKEL software [39]. The

Table 1 Experimental and theoretical values of the 1,2,4-trioxane ring parameters in artemisinin (bond lengths in Å; bond angles and torsional angles in degrees)

	Theoretical			Experimental[d]	Experimental[e]
Parameters[a]	3–21G [b]	3–21G**[c]	6–31G[c]		
O1–O2	1.462	1.462	1.447	1.475(4)	1.469(2)
O2–C3	1.440	1.440	1.435	1.417(4)	1.416(3)
C3–O4	1.436	1.436	1.435	1.448(4)	1.445(2)
O4–C5	1.407	1.408	1.403	1.388(4)	1.379(2)
C5–C6	1.529	1.530	1.533	1.528(5)	1.523(2)
C6–O1	1.477	1.477	1.469	1.450(4)	1.461(2)
O1–O2–C3	107.101	107.070	108.800	107.600(2)	108.100(1)
O2–C3–O4	107.279	107.310	106.760	107.200(2)	106.600(2)
C3–O4–C5	115.674	115.700	117.300	113.500(3)	114.200(2)
O4–C5–C6	112.086	112.030	112.280	114.700(2)	114.500(2)
C5–C6–O1	111.576	111.589	110.910	111.100(2)	110.700(2)
C6–O1–O2	111.296	111.286	113.240	111.500(2)	111.200(2)
O1–O2–C3–O4	−74.671	−74.680	−71.840	−75.500(3)	−75.500(2)
O2–C3–O4–C5	32.304	32.150	33.390	36.300(4)	36.000(2)
C3–O4–C5–C6	28.274	28.400	25.320	24.800(4)	25.300(2)
O4–C5–C6–O1	−50.854	−50.769	−49.410	−50.800(4)	−51.300(2)
C5–C6–O1–O2	9.991	9.792	12.510	12.300(3)	12.700(2)
C6–O1–O2–C3	50.330	50.522	46.700	47.700(3)	47.800(2)

[a] Atoms are numbered according to compound **1** in Fig. 1
[b] This work
[c] Values from Ref. [35]
[d] Values from Ref. [36] (experimental estimated standard deviations in brackets)
[e] Values from Ref. [37] (experimental estimated standard deviations in brackets)

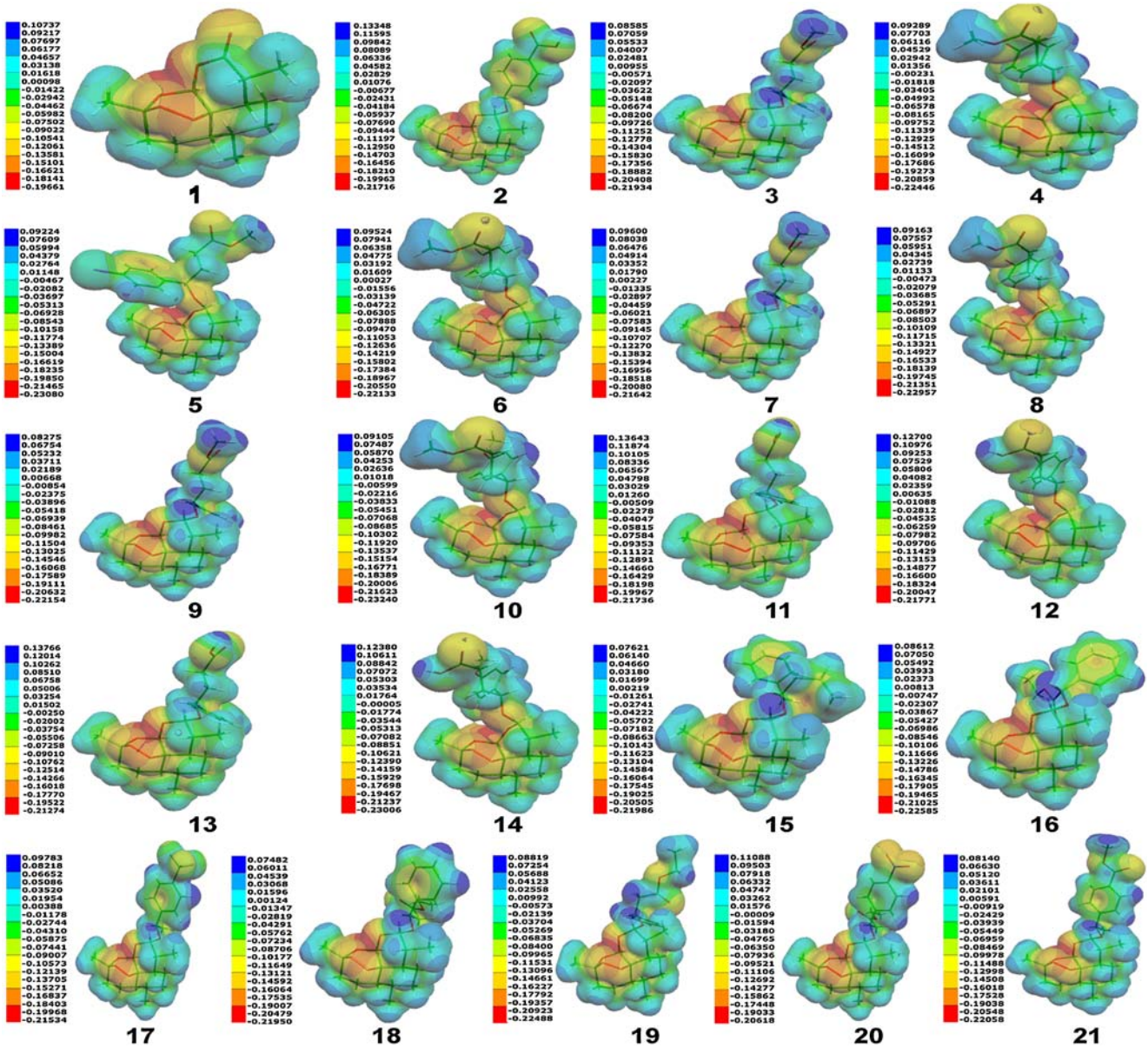

Fig. 3 MEP (values in au) maps of artemisinin and derivatives with antimalarial activity against D-6 strains of *P. falciparum*

portions of the surface with the most negative MEP values (red color) are found near the trioxane ring involved in the heme complex.

Molecular descriptors

In the descriptions of the structural characteristics of compounds **1** to **41** used to obtain valuable information about the influence of electronic, steric and hydrophobic features that allow us to quantify the biological activity of the molecules studied, we considered quantum descriptors [bond distances, bond and torsion angles, total energy, highest occupied molecular orbital (HOMO) energy, lowest unoccupied molecular orbital (LUMO) energy, Mulliken's electronegativity, molecular hardness, etc.]. With the purpose of representing different sources of chemical information in terms of molecular size and shape, symmetry and atom distribution in the molecule, we also included holistic molecular descriptors. Molecular volume (VOL), molecular refractivity, and octanol–water partition coefficient descriptors were also considered.

The quantum descriptors were obtained with the Gaussian 98 program. The holistic descriptors were generated with the WHIM-3D program [40] and the other descriptors were obtained with the ChemPlus module [41].

Multivariate analysis

All multivariate analyses were performed with the Pirouette program [42].

Table 2 Molecular parameters of training set compounds selected for partial least squares (PLS) analysis, experimental log relative activity (RA)[a] and the correlation matrix. *HOMO* Highest occupied molecular orbital, *VOL* molecular volume, *HYF* hydrophilic index

Compound	HOMO (hartree)	Q_1	Q_3	VOL (Å^3)	HYF	log RA (D-6)
1	−0.412	−0.3634	0.5418	759,95	−0.738	0.000
2	−0.350	−0.3615	0.5455	1107,80	−0.346	−0.017
3	−0.347	−0.3613	0.5454	1308,32	−0.758	0.637
4	−0.333	−0.3639	0.5478	1301,79	−0.758	0.731
5	−0.334	−0.3671	0.5467	1290,37	−0.758	1.000
6	−0.328	−0.3643	0.5482	1263,71	−0.758	0.958
7	−0.343	−0.3613	0.5457	1269,90	−0.758	0.803
8	−0.322	−0.3652	0.5480	1318,96	−0.758	0.765
9	−0.335	−0.3622	0.5453	1325,61	−0.758	0.588
10	−0.300	−0.3654	0.5489	1331,08	−0.765	0.675
11	−0.348	−0.3612	0.5452	1249,21	−0.349	0.212
12	−0.329	−0.3644	0.5480	1204,45	−0.349	0.248
13	−0.344	−0.3613	0.5456	1210,44	−0.349	0.225
14	−0.301	−0.3655	0.5487	1271,65	−0.360	0.011
15	−0.330	−0.3606	0.5464	1202,65	−0.831	0.605
16	−0.337	−0.3639	0.5501	1200,38	−0.774	0.885
17	−0.362	−0.3609	0.5452	1153,35	−0.743	0.429
18	−0.331	−0.3621	0.5457	1261,91	−0.781	0.897
19	−0.332	−0.3609	0.54610	1254,81	−0.781	0.930
20	−0.368	−0.3617	0.5437	1320,24	−0.717	0.842
21	−0.345	−0.3612	0.5459	1212,40	−0.774	0.628
HOMO		−0.408	0.839	0.744	0.067	0.280
Q_1			−0.537	−0.133	−0.002	−0.123
Q_3				0.519	0.003	0.317
VOL					−0.111	0.563
HYF						−0.758

[a] RA=IC_{50} of artemisinin/IC_{50} of analogue

Principal components analysis

The underlying purpose of principal components analysis (PCA) is dimension reduction. The use of this method produces a new set of variables called principal components (PCs), which is a linear combination of all the initial variables so that the first new variable (PC1) describes the largest variance in the data set, the second new variable (PC2) chosen must be orthogonal (uncorrelated) to the first, and in a direction such that it describes as many variances left as possible, and so on [31, 32].

Hierarchical cluster analysis

The primary purpose of hierarchical cluster analysis (HCA) is to display the data set in such a way as to emphasize its natural clusters and patterns in two-dimensional space. The distances between samples or variables that appear in the dendograms are calculated and compared through the similarity index, which ranges from 0 (i.e., no similarity and large distance among samples) to 1, for identical samples [31, 32].

Partial least squares analysis

In PLS analysis, a regression model was built between the X block of independent variables (given by the descriptors) and the Y vector (given by the activities). PLS is a projection method that uses projection of the matrix X onto a lower dimensional orthogonal basis, or at least a linear independent set [31–33].

Validation of the PLS model

The PLS model is validated through a cross-validation procedure (the leave-one-out technique) in order to verify the accuracy of the model in future predictions. The usefulness of the model is checked by SEP (Standard Error of Prediction), R^2 (correlation between the estimated values found by the model built with the full data set and actual values of y), Q^2 (crossvalidated correlation coefficient), and PRESS (predicted residual error sum of squares) parameters as well as the F-test.

Autoscaling

The purpose of autoscaling is to allow variables to be compared to each other on the same scale. In applying autoscaling, the data matrix was mean-centered followed by division by the standard deviation (autoscaling to unit variance).

Results and discussion

MEP maps

The MEP maps of artemisinin and artemisinin derivatives (**1**–**21**) are shown in Fig. 3. From this figure we can see that compounds (**2**–**21**) have similar MEP to artemisinin (**1**) around the essential trioxane ring.

To obtain the new artemisinins (**22**–**41**), we used the information reported by Lin et al. [30], and then considered the fact that a small methyl group substituted at the α-methylene carbon (*C) shows weaker activity than compounds with a larger carbethoxyalkyl substituent, which would increase the steric effect of the molecules and, concomitantly, their antimalarial activity. Compounds with electron-withdrawing function also substantially increase antimalarial activity.

The MEP maps to the new artemisinins (**22**–**41**) are shown in Fig. 4. In this figure, one can see that, around the essential 1,2,4-trioxane ring, the proposed compounds also present similar MEP to artemisinin (**1**).

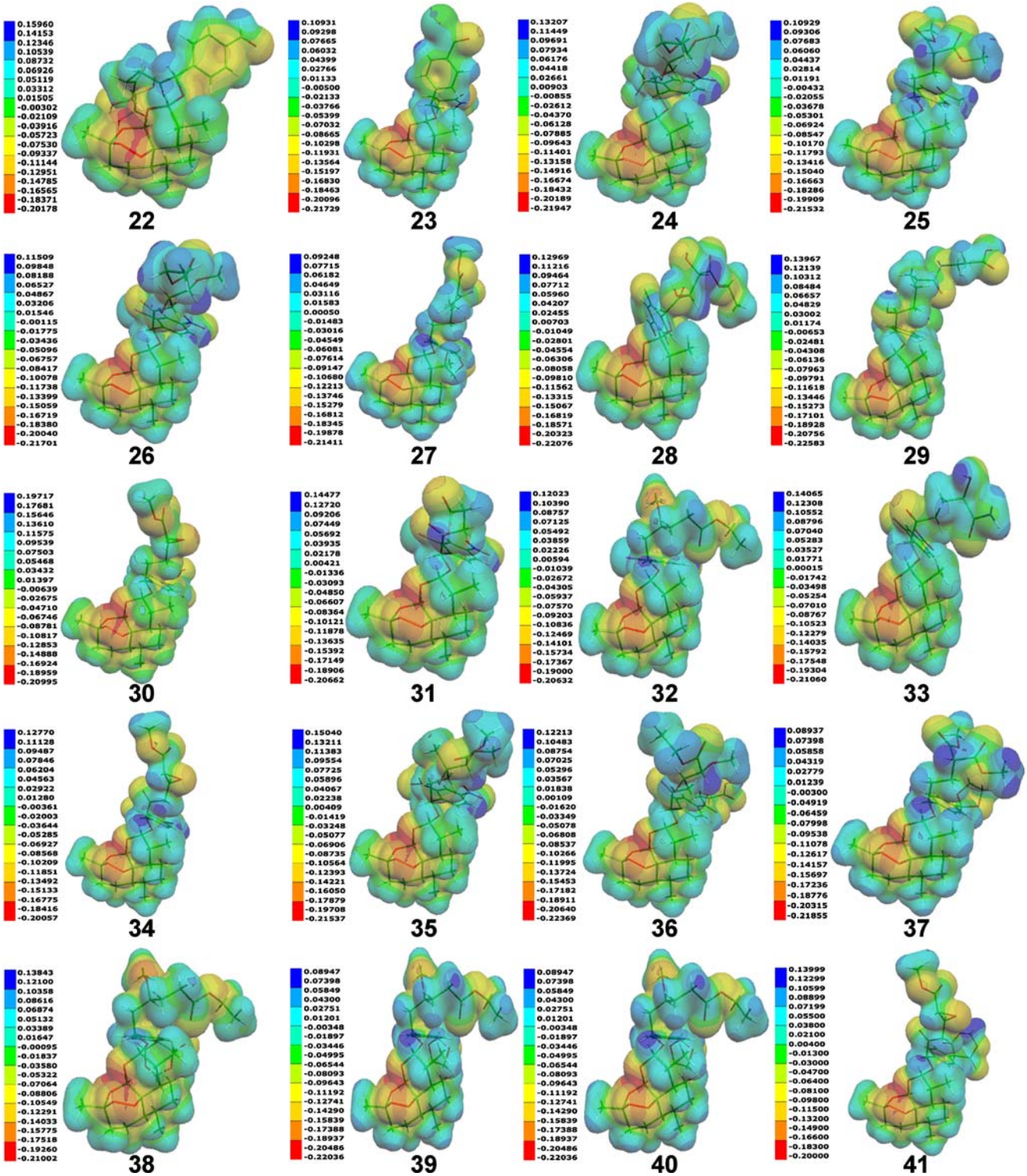

Fig. 4 MEP (au) maps to new proposed artemisinin derivatives with unknown antimalarial against D-6 strains of *P. falciparum*

Principle components and hierarchical cluster analysis

The analysis was started with 200 molecular descriptors and, in order to give each variable an equal weight in the analysis before applying the PCA, HCA, and PLS methods, each variable was auto-scaled. The selection of descriptors was done by PCA through matrix correlation of the variables, and those that showed little correlation with activity (<0.20, exception Q_1) were discarded. The PLS model was then built with descriptors that in general supply larger regression vectors (>0.20, exception Q_1 and Q_3).

Analysis of the data facilitated the selection of five descriptors. Table 2 shows the descriptors (HOMO, Q_1, Q_3, VOL, and HYF), the activity values of the antimalarial artemisinin derivatives, and correlations—including all data for 21 compounds. For the descriptors the correlation is less than 0.84, as can be seen in Table 2. The results of the selection for the first three PCs explained 91.7% of the total variance for the first 21 molecules from the training set. Figures 5 and 6 show the PC1–PC2 scores and loadings plots. From Fig. 5, one can see that PC2 discriminates between the most active (**3–9**, **10**, **15–21**) and the least active (**1**, **2**, **11–14**) compounds. According to Fig. 6, the most active compounds have the main contribution of HOMO, Q_1, Q_3, and VOL in the first principal component, while the least active compounds have a major contribution of the HYF descriptor in PC2.

The results of the HCA are displayed in the dendogram in Fig. 7 and are similar to those of PCA. The compounds are fairly well grouped according to their activity. From Fig. 7 one can see that the two clusters (+ and −) mirror the same two classes determined by PCA (Fig. 5).

PLS modeling

To build the PLS model, 15 compounds (n=15, calibration set) were used. Three latent variables (LVs) sproved significant: the explained variance (%EV) is 88.9% of the total variance, the correlation coefficient (R) is 0.967, and F (5,10)=25.892. Figure 8 shows the plot of the correlation between the measured and predicted logRA for the three LVs model, with the highly active compounds located in its lower part. The quality of the PLS model can be seen by numerical comparison between the measured and predicted activities listed in Table 3 and by Q^2, R^2, and SEP. From Table 3, it can be seen that the agreement between measured and predicted values is quite satisfactory; taking into account the complex molecular structure of artemisinin. The parameters considered as criteria for explaining the performance of the PLS model are quite meaningful (Q^2= 0.839, R^2=0.935).

$$\log RA = 0.2105HOMO + 0.024Q_1 + 0.1976Q_3 + 0.261VOL - 0.7006HYF$$

$$n = 15 \quad \%EV = 88.9 \quad R^2 = 0.935 \quad F_{(5,10)} = 25.8926$$

$$Q^2 = 0.839 \quad SEP = 0.152 \quad PRESS = 0.347$$

Table 4 shows the predicted activities against D-6 strains of *P. falciparum* resulting from application of the regression model.

For the compounds in the test set, the results showed that the increase in the steric effect in the α-methylene carbon (*C) characterized by the introduction of substituents in this carbon or in the benzene ring in the position ortho to the methylene group reflects the increase in antimalarial activity predicted by the PLS model.

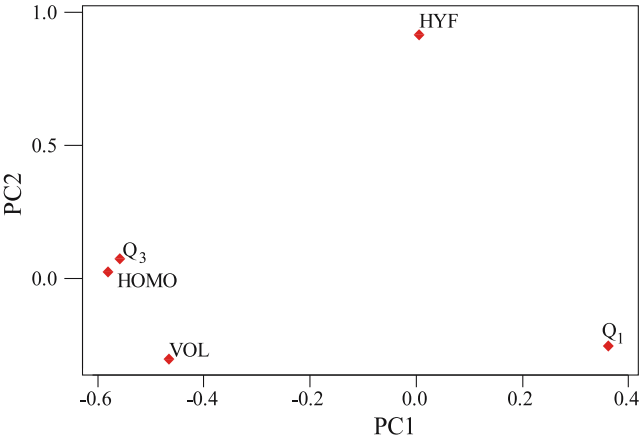

Fig. 6 Plot of the PC1–PC2 loadings obtained with the four descriptors selected to build the PLS model of artemisinin and derivatives with activity against D-6 strains of *P. falciparum*

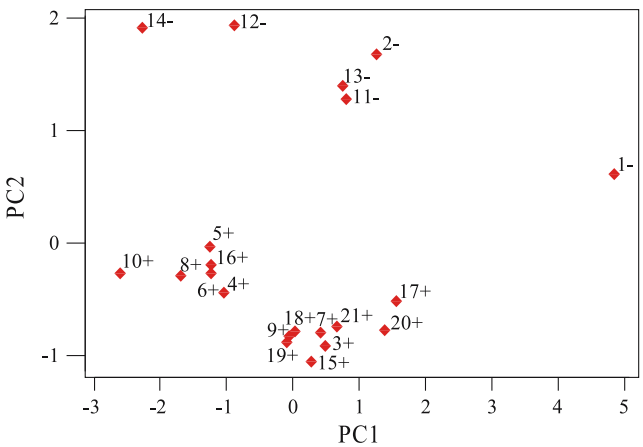

Fig. 5 Plot of the PC1–PC2 scores for artemisinin and derivatives. + Most active, − less active in activity against D-6 strains of *P. falciparum*

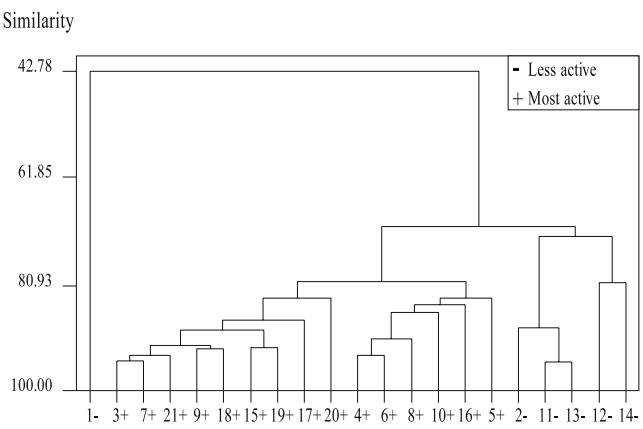

Fig. 7 Hierarchical cluster analysis (HCA) dendogram for artemisinin and derivatives with activity (+ most active; − less active) against D-6 strains of *P. falciparum*

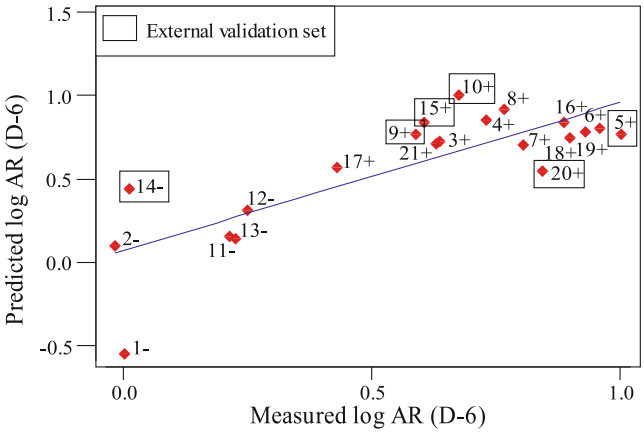

Fig. 8 Measured versus predicted log RA by PLS model using three latent variables (LVs). Symbols as in Fig. 5

For compounds in the test set predicted as less active (**22**, **23**, **28**, **30**, **33**), small substituent groups in R_3 and R_6 did not contribute to the increase in the molecular volume, thereby diminishing the antimalarial activity. However, for compounds (**27**, **37**–**41**) with large substituent groups in R_6, we noticed an increase in the molecular volume and, consequently, an increase in antimalarial activity. The results of predictions for compounds in the test set reveal that compounds (**25**, **27**, **37**, **38** and **40**) have predicted activities greater than that of artemisinin and some of the most potent derivatives in the training set (**3**, **4**, **7**, **8** and **21**).

Thus, information from QSAR models in combination with MEP maps can provide valuable insight into the experimental processes of syntheses and biological evaluation of the studied compounds.

Table 3 Experimental and estimated antimalarial activity (log RA) by PLS[a]

Compound	Antimalarial activity (log RA) Measured	Residuals Predicted	Experimental-predicted
1	0.000	−0.552	0.552
2	−0.017	0.100	−0.118
3	0.637	0.729	−0.092
4	0.731	0.851	−0.120
5[b]	1.000	0.769	0.231
6	0.958	0.806	0.152
7	0.803	0.702	0.101
8	0.765	0.920	−0.156
9[b]	0.588	0.769	−0.180
10[b]	0.675	1.007	−0.332
11	0.212	0.153	0.059
12	0.248	0.314	−0.066
13	0.225	0.143	0.082
14[b]	0.011	0.440	−0.429
15[b]	0.605	0.843	−0.238
16	0.885	0.838	0.048
17	0.429	0.567	−0.139
18	0.897	0.749	0.148
19	0.930	0.780	0.150
20[b]	0.842	0.545	0.297
21	0.628	0.712	−0.084

[a] PLS model using three principal components and leave-one-out cross-validation
[b] Samples from the external validation set

Table 4 Predicted antimalarial activity (log RA) of the compounds in Fig. 2 according to the PLS model

Compound	log RA
22	−1.132
23	0.296
24	0.248
25	0.763
26	0.311
27	0.965
28	−0.407
29	−0.906
30	0.105
31	−0.085
32	0.668
33	−0.642
34	0.536
35	0.146
36	−0.122
37	0.937
38	0.885
39	1.025
40	0.782
41	0.652

Conclusions

MEP maps were built for 21 compounds reported in the literature with antimalarial activity against D-6 strains of *Plasmodium falciparum*. Key features of the molecules that are necessary for their antimalarial activity together with chemical intuition allowed the introduction of substituents in derivatives of artemisinin to obtain 20 new artemisinins active against the malaria *falciparum*.

For the antimalarials reported in the literature, a significant regression model was obtained using the PLS method, based on the HOMO energy, charge Q_1 (O1), charge Q_3 (C3), molecular volume (VOL), and hydrophilic index (HYF). The regression model showed statistical significance and revealed that higher values for the HOMO energy combined with lower negative charge on the atom O1 (Q_1), higher positive charge on the atom C3 (Q_3), higher values for the VOL, and generally lower values for the HYF, increase antimalarial activity against *P. falciparum*. The use of the QSAR model along with MEP maps can provide valuable insights during

the experimental processes of syntheses and biological evaluation of the studied compounds.

Acknowledgments We gratefully acknowledge the financial support of the Brazilian agencies Conselho Nacional de Desenvolvimento Científico e Tecnológico and Coordenação de Aperfeiçoamento de Pessoal de Nível Superior. The authors would like to thank the Instituto de Química-Araraquara for the use of the GaussView software, and the Swiss Center for Scientific Computing for the use of the MOLEKEL software. We employed computing facilities at the Centro Nacional de Processamento de Alto Desempenho-Universidade Estadual de Campinas and at the Laboratório de Química Teórica e Computacional-Universidade Federal do Pará.

References

1. Bowman S, Lawson D, Basham D, Brow D, Chillingworth T, Churcher CM, Craig A, Davies RM, Devlin K, Feltwell T, Gentles S, Gwillinam R, Hamlin N, Harris D, Holroyd S, Hornsby T, Horrocks P, Jagels K, Jassal B, Kyes SJ, McLean S, Moule S, Mungall K, Murphy L, Olive RK, Quail MA, Rajadream M-A, Rutter S, Skelton J, Squares R, Squares S, Sulston JE, Whitehead S, Woodward JR, Newbold C, Barrell BG (1999) Nature 400:532–538
2. Pandey AV, Tekwani BL, Singh RL, Chaudan SV (1999) J Biol Chem 274:19383–19388
3. Kamchonwonggpaisan S, Samoff E, Meschinck SR (1997) Mol Biochem Parasitol 86:179–186
4. Olliaro P (2001) Pharmacol Ther 89:207–219
5. Ridley RG (2002) Nature 415:686–692
6. White NJ (2004) J Clin Invest 113:1084–1092
7. Arav-Boger R, Shapiro TA (2005) Annu Rev Pharmacol Toxicol 45:565–585
8. Cheng F, Shen J, Luo X, Zhu W, Gu J, Ji R, Jiang H, Chen K (2002) Bioorg Med Chem 10:2883–2891
9. Bhattacharjee AK, Hartell MG, Nichols DA, Hicks RP, Stanton B, van Hamont JE, Milhous WK (2004) Eur J Med Chem 39:59–67
10. Jefford CW (2001) Curr Med Chem 8:1803–1826
11. Haynes RK, Vonwiller SC (1997) Acc Chem Res 30:73–79
12. Bernardinelli G, Jefford CW, Maric D, Thomson C, Weber J (1994) Int J Quant Chem: Quant Biol Symp 21:117–131
13. Posner GH, Cumming JN, Ploypradith P, Oh CH (1995) J Am Chem Soc 117:5885–5886
14. Posner GH, Wang D, Cumming JN, Oh CH, French AN, Bodley AL, Shapiro TA (1995) J Med Chem 38:2273–2275
15. Haynes RK, Vonwiller SC (1996) Tetrahedron Lett 37:253–256
16. Rafiee MA, Hadipour NL, Naderi-manesh H (2005) J Chem Inf Model 45:366–370
17. Wu WM, Wu YK, Wu YL, Yao ZJ, Zhou CM, Li Y, Shan F (1998) J Am Chem Soc 120:3316–3325
18. Meshnick SR (2002) Int J Parasitol 32:1655–1660
19. Hynes RK, Krishna S (2004) Microb Infect 6:1339–1346
20. Kannan R, Kumar K, Sahal D, Kukreti S, Chauhan VS (2005) Biochem J 385:409–418
21. Kamchonwongpaisan S, Samoff E, Meschinck SR (1997) Mol Biochem Parasitol 86:179–186
22. Hon YL, Yang YZ, Meschnick SR (1998) Mol Biochem Parasitol 63:121–128
23. Wang DY, Wu YL (2000) Chem Commun 22:2193–2194
24. Hynes RK, Ho W-Y, Chen H-W, Fugmann B, Stetter J, Croft SL, Vivas L, Peters W, Robinson BR (2004) Angew Chem Int Ed 43:1381–1385
25. Hynes RK (2005) Angew Chem Int Ed 44:2064–2065
26. Pinheiro JC, Kiralj R, Ferreira MMC, Romero OAS (2003) QSAR Comb Sci 22:830–842
27. Roothaan CCJ (1951) Rev Mod Phys 23:69–89
28. Binkley JS, Pople JA, Hehre WJ (1980) J Am Chem Soc 102:939–946
29. Lin AJ, Zikry AB, Kyle DE (1997) J Med Chem 40:1396–1400
30. Lin AJ, Miller RE (1995) J Med Chem 38:764–770
31. Beebe KR, Pell JR, Seasholtt MB (1998) Chemometrics: a pratical guide. Wiley, New York, pp 81–278
32. Ferreira MMC (2002) J Braz Chem Soc 13:742–753
33. Kubinyi H (1993) QSAR: Hansch analysis and related approaches. In: Mannhold R, Krogsgaard-Larsen P, Timmerman H (eds) Methods and principles in medicinal chemistry, vol 1. VHC, Weinheim, pp 1–240
34. GaussView 1.0 (1997) Gaussian Inc., Pittsburgh, PA
35. Pinheiro JC, Ferreira MMC, Romero OAS (2001) J Mol Struct (Theochem) 572:35–44
36. Leban I, Golic L, Japelj M (1998) Acta Pharm Jugosl 38:71–77
37. Lisgarten JN, Potter BS, Bantuzeko C, Palmer RA (1998) J Chem Cryst 28:539–543
38. Frisch MJ, Trucks GW, Schlegel HB, Scuseria GE, Millam MA, Daniels AD, Kudin KN, Strain MC, Farkas O, Tomasi Barone JV, Cossi M, Cammi R, Mennucci B, Pomelli C, Adamo C, Clifford S, Ochterski J, Petersson GA, Ayala PY, Cui Q, Morokuma K, Salvador P, Dannenberg JJ, Malick DK, Rabuck AD, Raghavachari K, Foresman JB, Cioslowski J, Ortiz JV, Baboul AG, Sefanov BB, Liu G, Liashenko A, Piskorz P, Komaromi I, Gomperts R, Martin RL, Fox DJ, Keith T, A-Laham MA, Peng CY, Nanayakkara A, Challacombe M, Gill PMW, Johnson B, Chen W, Wong MW, Andes JL, Gonzalez C, Head-Gordon M, Replogle ES, Pople JA (2001) Gaussian 98 - Revision A.11. Gaussian Inc, Pittsburgh PA
39. Flukiger P, Luthi HP, Portmann S, Weber J (2000–2001) MOLEKEL. Swiss Center for Scientific Computing, Mano, Switzerland
40. Todeschine R, Gramatica P (1997) WHIM-3D 3.3. Milan
41. ChemPlus (2000) Modular extensions to hyperChem release 6.02, molecular modeling for windows. HyperCube Inc, Gainesvillem FL
42. Infometrix, Pirouette 3.01, Woodinville WA, 2001